Competitive Mechanisms and Origins of Stereocontrol in the [2 + 2] Thermal Cycloaddition between Imines and Keteniminium Cations. A Complementary Entry to 2-Azetidinones (β-Lactams) and Related Compounds

Ana Arrieta and Fernando P. Cossío*

Kimika Fakultatea, Euskal Herriko Unibertsitatea, P.K. 1072, 20080 San Sebastián-Donostia, Spain

Begoña Lecea

Farmazi Fakultatea, Euskal Herriko Unibertsitatea, P.K. 450, 01080 Vitoria-Gasteiz, Spain

Received July 28, 1998

The different reaction paths associated with the formal [2 + 2] thermal cycloaddition between several keteniminium cations and imines has been studied computationally. It is found that the reaction takes place via stepwise mechanisms that involve the sequential formation of the N1−C2 and the C3−C4 bonds. In some cases, the second step of the reaction is subjected to torquoelectronic effects and determines its stereochemical outcome. Under these conditions, preferential or exclusive formation of cis cycloadducts is predicted, in good agreement with part of the experimental evidence available. When chloroenamines are used as precursors of the keteniminium ions, the step in which the C3−C4 bond is formed can consist of an intramolecular S_N2 reaction. Under these conditions, the stereocontrol of the reaction is significantly lower and the trans isomer is preferentially formed. According to our results, generation of keteniminium cations from enamines having good leaving groups is recommended to improve the stereocontrol of the reaction.

Introduction

One of the most distinctive properties of cumulenes is their ability to participate in [2 + 2] thermal cycloadditions.[1] Although these reactions have been known since 1907,[2] they have fascinated both theoretical and experimental chemists for decades, since the four-membered cycloadducts thus formed are of preparative interest[3] and, in addition, the mechanism of these reactions is intellectually challenging.[1,4] The [2 + 2] cycloaddition chemistry of ketenes and allenes has been extensively studied by different groups,[5] including our own.[6] In sharp contrast, the mechanism of the cycloadditions between neutral or cationic azacumulenes (namely, ketenimines and keteniminium salts) and π-systems has been scarcely explored.[7,8] Among the two studies reported so far, both deal with the interaction between neutral iminoketenes and carbonyl compounds. Quite surprisingly, the mechanism of the [2 + 2] cycloaddition reaction between azacumulenes and imines remains completely unexplored. However, these reactions are of great practical significance, since they constitute an alternative to the Staudinger reaction[9] between ketenes and imines to yield 2-azetidinones (β-lactams), whose importance in the chemical synthesis of antibiotics[10] and other biologically interesting compounds[11] is well recognized.

The most studied [2 + 2] cycloaddition between azacumulenes and imines is one that involves keteniminium

(1) (a) Tidwell, T. T. *Ketenes*; Wiley: New York, 1995; pp 460−536. (b) Hyatt, J. A.; Raynolds, P. W. *Org. React.* **1994**, *45*, 159.

(2) (a) Staudinger, H. *Chem. Ber.* **1907**, *40*, 1145. (b) Wilsmore, N. T. M. *J. Am. Chem. Soc.* **1907**, *91*, 1937.

(3) See, for example: (a) Snider, B. B. *Chem. Rev.* **1988**, *88*, 793. (b) Pommier, A.; Pons, J.-M. *Synthesis* **1993**, 441. (c) Pommier, A.; Pons, J.-M. *Synthesis* **1995**, 729. (d) Oligaruso, M. A.; Wolfe, J. F. In *Synthesis of Lactones and Lactams*; Patai, S., Rappoport, Z., Eds.; Wiley: Chichester, 1993.

(4) (a) Woodward, R. B.; Hoffmann, R. *The Conservation of Orbital Symmetry*; Academic: New York, 1971. (b) Fleming, I. *Frontier Orbitals and Organic Chemical Reactions*; Wiley: Chichester, 1976. (c) Houk, K. N.; Li, Y.; Evanseck, J. D. *Angew. Chem., Int. Ed. Engl.* **1992**, *31*, 682. (d) Houk, K. N.; González, J.; Li, Y *Acc. Chem. Res.* **1995**, *28*, 81.

(5) (a) Wang, X.; Houk, K. N. *J. Am. Chem. Soc.* **1990**, *112*, 1754. (b) Sordo, J. A.; González, J.; Sordo, T. L. *J. Am. Chem. Soc.* **1992**, *114*, 6249. (c) López, R.;. Sordo, T. L.; Sordo, J. A.; González, J. *J. Org. Chem.* **1993**, *58*, 7036. (d). Assfeld, X.; Ruiz-López, M. F.; González, J.; López, R.; Sordo, J. A.; Sordo, T. L. *J. Comput. Chem.* **1994**, *15*, 479. (e) López, R.; Ruiz-López, M. F.; Rinaldi, D.;. Sordo, J. A.; Sordo, T. L. *J. Phys. Chem.* **1996**, *100*, 10600. (f) Cooper, R. D. G.; Daugherty, B. W.; Boyd, D. B. *Pure Appl. Chem.* **1987**, *59*, 485. (g) Pons, J.-M.; Pommier, A.; Rajzmann, M.; Liotard, D. *THEOCHEM* **1994**, *313*, 361. (h) Pons, J.-M.; Oblin, M.; Pommier, A.; Rajzmann, M.; Liotard, D. *J. Am. Chem. Soc.* **1997**, *119*, 3333. (i) Yamabe, S.; Minato, T.; Osamura, Y. *J. Chem. Soc., Chem. Commun.* **1993**, 450. (j) Seidl, E. T.; Schaeffer, H. F., III. *J. Am. Chem. Soc.* **1991**, *113*, 5195. (k) Schaad, L. J.; Gutman, I.; Hess, B. A., Jr.; Hu, J. *J. Am. Chem. Soc.* **1991**, *113*, 5200. (l) Valentí, E.; Pericàs, M. A.; Moyano, A. *J. Org. Chem.* **1990**, *55*, 3582. (m) Yamabe, S.; Dai, T. S.; Minato, T.; Machiguchi, T.; Hasegawa, T. *J. Am. Chem. Soc.* **1996**, *118*, 6518. (n) Salzner, V.; Bacharach, S. M. *J. Org. Chem.* **1996**, *61*, 237.

(6) (a) Cossío, F. P.; Ugalde, J. M.; Lopez, X.; Lecea, B.; Palomo, C. *J. Am. Chem. Soc.* **1993**, *115*, 995. (b) Cossío, F. P.; Arrieta, A.; Lecea, B.; Ugalde, J. M. *J. Am. Chem. Soc.* **1994**, *116*, 2085. (c) Lecea, B.; Arrieta, A.; Roa, G.; Ugalde, J. M.; Cossío, F. P. *J. Am. Chem. Soc.* **1994**, *116*, 9613. (d) Lecea, B.; Arrieta, A.; Lopez, X.; Ugalde, J. M.; Cossío, F. P. *J. Am. Chem. Soc.* **1995**, *117*, 12314. (e) Lecea, B.; Arrastia, I.; Arrieta, A.; Roa, G.; Lopez, X.; Arriortua, M. I.; Ugalde, J. M.; Cossío, F. P. *J. Org. Chem.* **1996**, *61*, 3070. (f) Lecea, B.; Arrieta, A.; Arrastia, I.; Cossío, F. P. *J. Org. Chem.* **1998**, *63*, 5216.

(7) Fabian, W. M. F.; Janoschek, R. *J. Am. Chem. Soc.* **1997**, *119*, 4253.

(8) Fang, D.-C.; Fu, X.-Y. *Chem. Phys. Lett.* **1996**, *259*, 265.

(9) (a) Staudinger, H. *Liebigs Ann. Chem.* **1907**, *356*, 51. (b) Hegedus, L. S.; Montgomery, J.; Narukawa, Y.; Snustad, D. C. *J. Am. Chem. Soc.* **1991**, *113*, 5784.

(10) (a) Thomas, R. C. In *Recent Progress in The Chemical Synthesis of Antibiotics*; Lukacs, G., Ohno, M., Eds.; Springer-Verlag: Berlin, 1989. (b) *Chemistry and Biology of β-Lactam Antibiotics*; Morin, R. B., Gorman, M., Eds.; Academic Press: New York, 1982; Vols. 1−3.

(11) (a) *The Organic Chemistry of β-Lactams*; Georg, G. L., Ed.; Verlag Chemie: New York, 1993. (b) Ojima, I. *Acc. Chem. Res.* **1995**, *28*, 383.

10.1021/jo9815002 CCC: $18.00
Published on Web 02/19/1999

Scheme 1. Reaction between Keteniminium Salts and Imines as a Convergent Approach for the Chemical Synthesis of 2-Azetidinones (*β*-Lactams)[a]

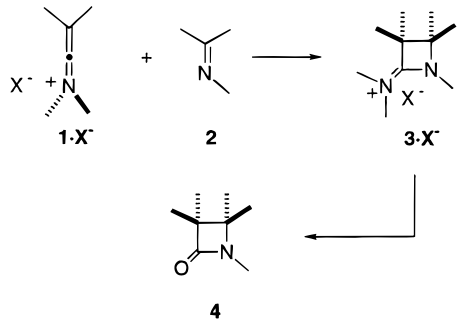

[a] In this and subsequent schemes, unless otherwise stated the possible substituents at the different positions are not specified.

salts. This reaction was discovered in 1974 by Ghosez et al.[12] and leads to the formation of 2-azetidinium salts (Scheme 1), which can in turn be converted into 2-azetidinones **4** or into other compounds, including amino acid derivatives.[13] This reaction has been explored by several groups, and its scope and more relevant features have been reviewed.[14] In principle, the reaction has two important advantages over the Staudinger reaction: First, keteniminium salts are very reactive electrophilic species and undergo cycloaddition reactions with imines even when the analogous ketenes remain unreactive. Second, the nitrogen atom of the keteniminium salt can incorporate chiral groups, and therefore, there is an additional position available to develop asymmetric versions of the reaction. Indeed, high chiral induction (up to 99% ee) has been achieved in some cases.[15] The main drawback of the reaction is, however, that a lower stereocontrol is usually obtained in comparison with that observed in the Staudinger reaction between ketenes and imines. In contrast with this latter reaction, trans selectivity is observed in many cases.[14] However, a recent paper from Battaglia et al.[16] has reported high cis stereoselectivity in the [2 + 2] cycloaddition between imines and keteniminium triflates.

Several qualitative models have been proposed to explain the experimental findings. These proposals vary according to the different experimental protocols usually followed to carry out the reaction. Keteniminium salts are usually generated in situ from carboxamides. Reaction of a given amide **5** with phosgene yields the corresponding α-chloroiminium chloride **6** (Scheme 2, X = Cl), which in the presence of a base yields the neutral chloroenamine **7**. This latter compound can equilibrate with the corresponding keteniminium salt **1·X**⁻. In fact,

Scheme 2. Generation of Keteniminium Salts from Carboxamides

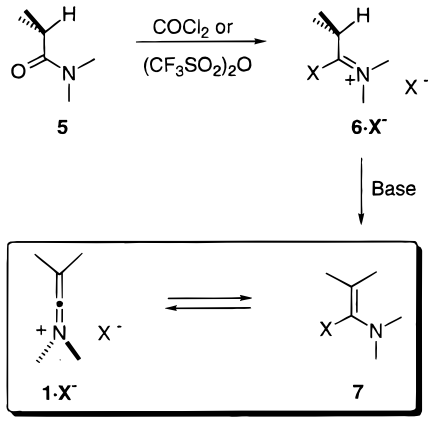

X=Cl or CF_3SO_3

Scheme 3. Possible Reaction Paths for the Formation of [2 + 2] Cycloadducts from Keteniminium or Iminium Salts

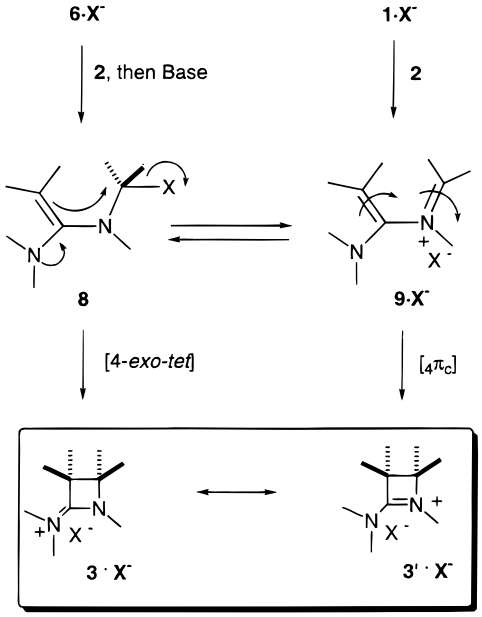

the high reactivity of chloroenamines **7** (X=Cl) toward nucleophiles was explained by Ghosez[12] on the basis of a fast preequilibrium between the **7** and **1·X**⁻ species, in which the keteniminium salt is the actual electrophile. More recently, Battaglia et al.[16] have prepared keteniminium triflates **1·X**⁻ (Scheme 2, X = CF_3SO_3) from the corresponding amides and triflic anhydride. These authors suggested that the **7** → **1·X**⁻ equilibrium is more shifted toward the keteniminium species than in the case of chloroenamines.

Both the **6** and **1** species can in principle react with a nucleophile, as represented in Scheme 3. Thus, the iminium salt **6** can react with the imine **2** in the presence of base to yield the intermediate **8**. This intermediate can form the corresponding four-membered ring **3** via a [*4-exo-tet*] intramolecular S_N2 displacement. Alternatively, keteniminium salt **1** (or its precursor **7**) can react with **2** to form the iminium salt **9**. This latter intermediate can form the product **3** ↔ **3′** via a conrotatory electrocyclic ring closure. Moreover, the **8** and **9** inter-

(12) De Poortere, M.; Marchand-Brynaert, J.; Ghosez, L. *Angew. Chem., Int. Ed. Engl.* **1974**, *13*, 267.

(13) (a) Marchand-Brynaert, J.; Moya-Portuguez, M.; Lesuisse, D.; Ghosez, L. *J. Chem. Soc., Chem. Commun.* **1980**, 173. (b) Marchand-Brynaert, J.; Moya-Portuguez, M.; Huber, I.; Ghosez, L. *J. Chem. Soc., Chem. Commun.* **1983**, 818.

(14) (a) Ghosez, L.; Marchand-Brynaert, J. In *Comprehensive Organic Synthesis*; Trost, B. M., Fleming, I., Paquette, L. A., Eds.; Pergamon Press: Oxford, 1991; Vol. 5, pp 85−122. (b) Ghosez, L.; Bogdan, S.; Cérésiat, M.; Frydrych, C.; Marchand-Brynaert, J.; Moya-Portuguez, M.; Huber, I. *Pure Appl. Chem.* **1987**, *59*, 393. (c) Ghosez, L. In *Organic Synthesis: Today and Tomorrow*; Trost, B., Hutchinson, C. R., Eds.; Pergamon Press: New York, 1981.

(15) These very promising results are based on iminium salts derived from (*2S*)-(methoxymethyl)pyrrolidine, and have been reported by the Ghosez's group. See ref 14a and footnote 222 therein.

(16) Barbaro, G.; Battaglia, A.; Bruno, C.; Giorgianni, P.; Guerrini, A. *J. Org. Chem.* **1996**, *61*, 8480.

mediates could equilibrate, as occurred in the case of the **7** and **1** species.

Within this context, we reasoned that modern computational tools could help to clarify the nature of the different reaction paths involved in this complex reaction. In addition, it is clear that an understanding of the mechanisms of this reaction and of the reasons that determine its stereochemical outcome would be of considerable practical utility, given the importance of the reaction products. Therefore, in this paper we present for the first time a computational study on the reaction between several simple keteniminium salts and imines to yield *cis*- and *trans*-2-azetidinium salts. Finally, we propose several models that could be useful in further experimental work on this important reaction.

Computational Methods

All the calculations included in this work have been performed with the GAUSSIAN 94 suite of programs.[17] All stationary points have been located at the HF/6-31G* level,[18] and energies have been recalculated at the second-order Møller−Plesset level[19] on previously fully optimized HF/6-31G* geometries and including zero-point vibrational energy corrections scaled by 0.89 as recommended.[20] These results are denoted as MP2/6-31G*//HF/6-31G*. In several cases, full optimizations at the MP2/6-31G* level have been carried out. Several reaction paths have been checked by intrinsic reaction coordinate (IRC) calculations[21] in order to verify that the located transition structures connect reactants, reaction intermediates, and products. All stationary points have been characterized by harmonic analysis.[22] Transition structures have one and only one negative eigenvalue in their diagonalized Hessian matrixes, associated with nuclear motion along the reaction coordinate under study. Density functional theory (DFT)[23] has also been used in order to include electron correlation in the course of the optimizations. The hybrid three-parameter functional developed by Becke (B3LYP)[24] has been used since this method has proven to yield very accurate results in other pericyclic reactions.[25] Frequency calculations have also been computed at the B3LYP/6-31G* level, and the ZPVE's have not been scaled.

Nonspecific solvent effects have been taken into account by using the self-consistent reaction field (SCRF) approach.[26] The solvation energies of cationic species have been calculated within the SCRF framework by means of the self-consistent isodensity polarization continuum model (SCIPCM).[27] In the case of neutral species, the Onsager approach[28] (denoted as L1A1[29]) has been used in geometry optimizations. The calculations reported in this work have been carried out for 1,2-dichloroethane ($\epsilon = 10.37$),[30] a very common solvent for this kind of reaction.

Wiberg bond indices[31] and atomic charges[32] have been computed using the natural population analysis[33] (NPA).

Chart 1

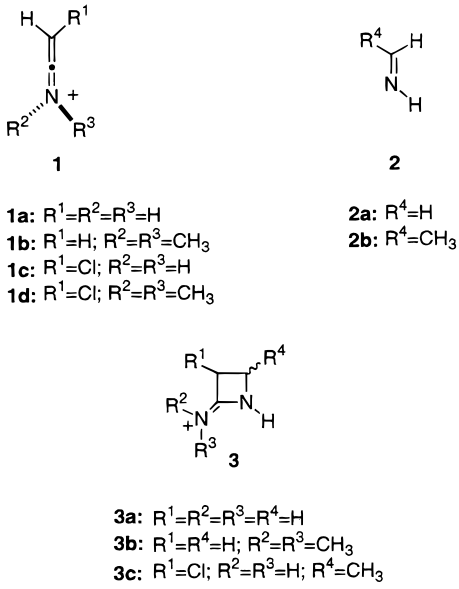

Results and Discussion

The reactants and products included in our study are collected in Chart 1. Inspection of the frontier molecular orbitals (FMO's) of the keteniminium cation **1a** (see Figure 1) reveals a MO composition and topology similar to that previously found for ketene.[6a] Thus, both FMO's lie in orthogonal planes, the LUMO being in the $H_2C{=}C$ plane, with a larger coefficient for the sp-hybridized carbon atom. Given the superior electrophilicity of the

(17) GAUSSIAN 94, Revision B.2: Frisch, M. J.; Trucks, G. W.; Schlegel, H. B.; Gill, P. M. W.; Johnson, B. G.; Robb, M. A.; Cheeseman, J. R.; Keith, T.; Peterson, G. A.; Montgomery, J. A.; Raghavachari, K.; Al-Laham, M. A.; Zakzrewski, V. G.; Ortiz, J. V.; Foresman, J. B.; Peng, C. Y.; Ayala, P. Y.; Chen, W.; Wong, M. W.; Andres, J. L.; Repogle, E. S.; Gomperts, R.; Martin, R. L.; Fox, D. J.; Binkley, J. S.; Defrees, D. J.; Baker, J.; Stewart, J. P.; Head-Gordon, M.; Gonzalez, C.; Pople, J. A. Gaussian, Inc.: Pittsburgh, PA, 1995.

(18) Hehre, W. J.; Radom, L.; Schleyer, P. v. R.; Pople, J. A. *Ab Initio Molecular Orbital Theory*; Wiley: New York; 1986; pp 65−88 and references therein.

(19) (a) Møller, C.; Plesset, M. S. *Phys. Rev.* **1934**, *46*, 618. (b) Pople, J. A.; Krishman, R.; Schlegel, H. B.; Binkley, J. S. *Int. J. Quantum Chem. Symp.* **1979**, *13*, 225.

(20) Pople, J. A.; Schlegel, H. B.; Krishnan, R.; DeFrees, D. J.; Binkley, J. S.; Frisch, H.; Whiteside, R.; Hout, R. F., Jr.; Hehre, W. J. *Int. J. Quantum Chem. Symp.* **1981**, *15*, 269.

(21) (a) Fukui, K. *Acc. Chem. Res.* **1981**, *14*, 363. (b) Gonzalez, C.; Schlegel, H. B. *J. Chem. Phys.* **1989**, *90*, 2154. (c) Gonzalez, C.; Schlegel, H. B. *J. Phys. Chem.* **1990**, *94*, 5523.

(22) McIver, J. W.; Komornicki, A. K. *J. Am. Chem. Soc.* **1972**, *94*, 2625.

(23) (a) Parr, R. G.; Yang, W. *Density-Functional Theory of Atoms and Molecules*; Oxford: New York, 1989. (b) Bartolotti, L. J.; Fluchick, K. In *Reviews in Computational Chemistry*; Lipkowitz, K. B., Boyd, D. B., Eds.; VCH Publishers: New York, 1996; Vol. 7, pp 187−216.

(24) (a) Becke, A. D. *J. Chem. Phys.* **1993**, *98*, 5648. (b) Becke, A. D. *Phys. Rev. A* **1988**, *38*, 3098. (c) Lee, C.; Yang, W.; Parr, R. G. *Phys. Rev. B* **1980**, *37*, 785. (d) Vosko, S. H.; Wilk, L.; Nusair, M. *Can. J. Phys.* **1980**, *58*, 1200.

(25) See, for example: (a) Wiest, O.; Black, K. A.; Houk, K. N. *J. Am. Chem. Soc.* **1994**, *116*, 10336. (b) Wiest, O.; Houk, K. N.; Black, K. A.; Thomas, B., IV. *J. Am. Chem. Soc.* **1995**, *117*, 8594. (c) Goldstein, E.; Beno, B.; Houk, K. N. *J. Am. Chem. Soc.* **1996**, *118*, 6036. (d) Branchadell, V. *Int. J. Quantum Chem.* **1997**, *61*, 381. (e) Deng, Q.; Thomas, B. E., IV; Houk, K. N.; Dowd, P. *J. Am. Chem. Soc.* **1997**, *119*, 6902.

(26) (a) Tomasi, J.; Persico, M. *Chem. Rev.* **1994**, *94*, 2027. (b) Simkin, B. Y.; Sheikhet, I. *Quantum Chemical and Statistical Theory of Solutions—A Computational Approach*; Ellis Horwood: London, 1995; pp 78−101. (c) Cramer, C. J.; Truhlar, D. G. In *Reviews in Computational Chemistry*; Lipkowitz, K. B., Boyd, D. B., Eds.; VCH Publishers: New York, 1995; Vol. VI, pp 1−72.

(27) (a) Wiberg, K. B.; Castejon, H.; Keith, T. A. *J. Comput. Chem.* **1996**, *17*, 185. (b) Wiberg, K. B.; Keith, T. A.; Frisch, M. J.; Murcko, M. *J. Phys. Chem.* **1995**, *99*, 9072. (c) Wiberg, K. B.; Rablen, P. R.; Rush, D. J.; Keith, T. A. *J. Am. Chem. Soc.* **1995**, *117*, 4261.

(28) (a) Onsager, L. *J. Am. Chem. Soc.* **1936**, *58*, 1486. (b) Wong, M. W.; Wiberg, K. B.; Fisch, M. J. *J. Am. Chem. Soc.* **1992**, *114*, 523. (c) Wong, M. W.; Wiberg, K. B.; Frisch, M. J. *J. Am. Chem. Soc.* **1992**, *114*, 1645.

(29) Morao, I.; Lecea, B.; Arrieta, A.; Cossío, F. P. *J. Am. Chem. Soc.* **1997**, *119*, 816.

(30) Reichardt, C. *Solvents and Solvent Effects in Organic Chemistry*; VCH Publishers: Weinheim, 1990; p 409.

(31) Wiberg, K. B. *Tetrahedron* **1968**, *24*, 1083.

(32) Wiberg, K. B.; Rabien, P. R. *J. Comput. Chem.* **1993**, *14*, 1504.

(33) a) Reed, A. E.; Curtiss, L. A.; Weinhold, F. *Chem. Rev.* **1988**, *88*, 899. (b) Reed, A. E.; Weinstock, R. B.; Weinhold, F. *J. Chem. Phys.* **1985**, *83*, 735.

Table 1. Energy Barriers (Δ*E*, kcal/mol) Computed for the Reaction between Keteniminium Cations 1a−c and Imines 2a,b to Form Cycloadducts 3a−c[a]

method	ΔE_1	ΔE_{a1}	ΔE_2	ΔE_{a2}	ΔE_{rxn}
			1a + 2a → 3a		
HF/6-31G*[b]	−21.89	+11.07	−16.97	+32.99	−63.20
MP2/6-31G*[b]	−26.81	+11.40	−18.82	+22.08	−70.96
B3LYP/6-31G*[c]	−31.88		−9.88	+21.27	−64.36
MP2/6-31G*[d]	−33.12		−12.32	+22.56	−71.08
			1b + 2a → 3b		
HF/6-31G*[b]	−10.88	+7.20	−11.82	+29.81	−54.09
MP2/6-31G*[b]	−12.43	+0.14	−17.78	+18.26	−62.68
B3LYP/6-31G*[c]	−10.80	+0.67	−14.41	+16.68	−55.18
B3LYP(SCIPCM)/6-31G*[c]	−4.78	+0.54	−23.61	+19.95	−56.24
			1c + 2b → *cis*-3c		
HF/6-31G*[b]	−25.12	+9.49	−24.04	+31.76	−67.22
MP2/6-31G*[b]	−30.92	+12.02	−25.71	+20.04	−77.11
			1c + 2b → *trans*-3c		
HF/6-31G*[b]	−25.12	+12.95	−24.60	+43.36	−68.03
MP2/6-31G*[b]	−30.92	+14.46	−26.16	+34.31	−77.52

[a] See Chart 1 and Figure 2 for the notation of the species and the energy barriers involved. [b] Geometries fully optimized at the HF/6-31G* level. The ZPVE corrections, computed at the same level and conveniently scaled, have been included. [c] Geometries fully optimized at the B3LYP/6-31G* level. The ZPVE corrections, computed at the same level, have been included. [d] Geometries fully optimized at the MP2/6-31G* level. The ZPVE corrections, computed at the same level and conveniently scaled, have been included.

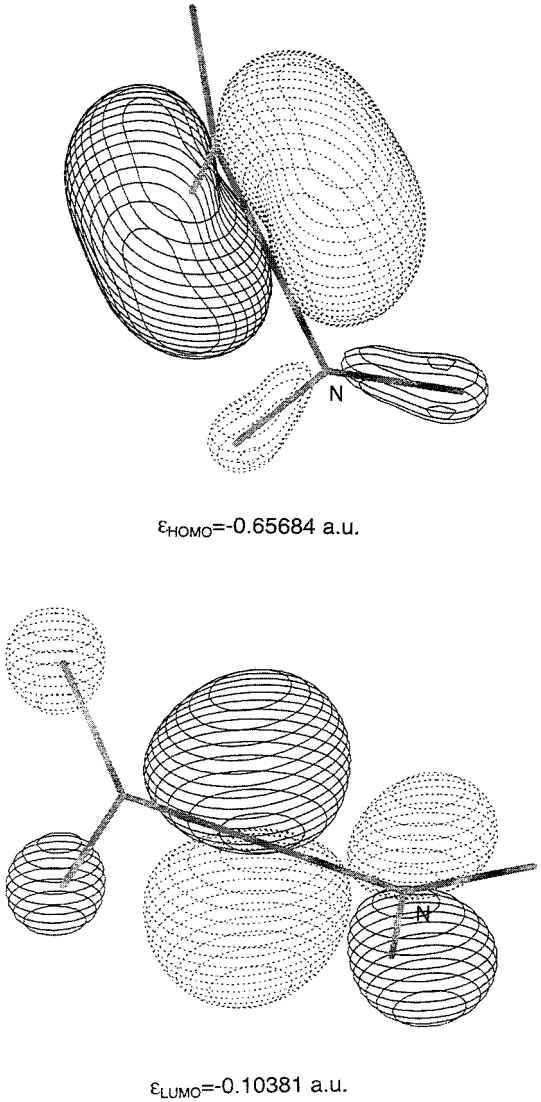

Figure 1. Computer plots of the frontier canonical orbitals of keteniminium cation **1a** computed at the B3LYP/6-31G* level. The orbital energies have been computed at the same level and are given in au.

keteniminium cations with respect to ketenes, it is expected that the reaction between **1a** and **2a** will take place through a nucleophilic attack of the iminic lone pair of electrons on the central carbon of **1a**. Indeed, all our attempts to locate concerted (although highly asynchronous) $[\pi^2_s+\pi^2_a]$ or $[\pi^2_s+(\pi^2_s+\pi^2_s)]$ mechanisms[34] were unfruitful. Instead, the reaction profile depicted in Figure 2 was found. Interaction between **1a** and **2a** yields first an ion−molecule intermediate denoted as **INT1a** in Figure 3. The complexation energy with respect to the reactants is found to be −26.81 kcal/mol at the MP2/6-31G*//HF/6-31G* level (see Table 1). However, part of this energy is caused by the hydrogen bond between the N5−H and the N1 groups. When this complex was reoptimized at either MP2/6-31G* or B3LYP/6-31G* levels, a proton transfer from the N5−H group to the N1 atom was obtained and the ΔE_1 value found was even higher at this level. Since in the experimental studies *N*,*N*-dimethyl keteniminium salts are used, this proton transfer and the high ΔE_1 values obtained for the **1a** + **2a** → **3a** reaction are not chemically relevant and the HF/6-31G* potential energy hypersurface describes more properly the reaction path (vide infra).

We located a saddle point associated with the N1−C2 bond formation. This transition structure is denoted as **TS1a** in Figure 2, and its geometrical features (see Figure 3) are those one can expect from the nucleophilic attack of the lone pair of electrons of N1 on the sp-hybridized C2 atom of **1a**, along the LUMO plane (see Figure 1). The low value of the bond index between N1 and C2 (B_{12} = 0.142, see Table 1 of the Supporting Information) of **TS1a** as well as the positive charge of the iminic fragment are consistent with a relatively early transition structure. Given that at the MP2/6-31G* and B3LYP/6-31G* levels the imine is protonated prior the formation of the N1−C2 bond, this transition structure could not be located at these levels. At the MP2/6-31G*//HF/6-31G* level, the activation energy associated with the N1−C2 bond is calculated to be 11.40 kcal/mol (Table 1).

We next located a second reaction intermediate denoted as **INT2a** in Figure 3. In this stationary point the N1−C2 bond is completely formed (B_{12} = 0.911; see Table 1 of the Supporting Information) and the interaction between C2 and C3 has a significant double-bond character (see Figure 1 of the Supporting Information). In addition, the MP2/6-31G* geometry is almost identical

(34) Pasto, D. J. *J. Am. Chem. Soc.* **1979**, *101*, 37.

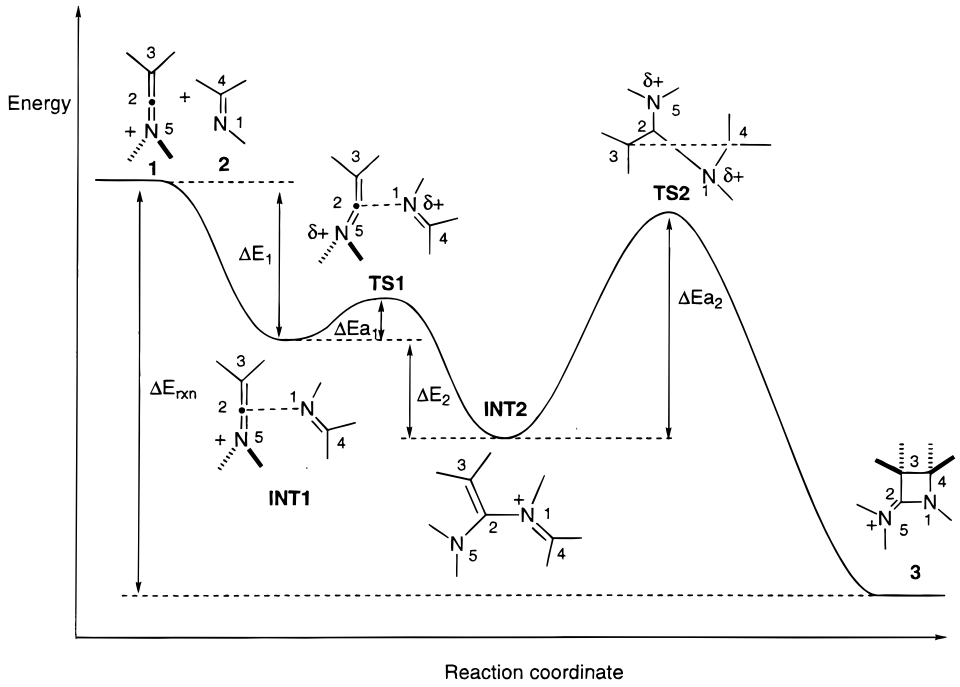

Figure 2. Qualitative reaction profile of the [2 + 2] reaction between keteniminium salts and imines. The possible substituents at the different positions are not specified.

Scheme 4. C−N, Bond Distances Found in the *COTNAA* Structure (See Ref 37)

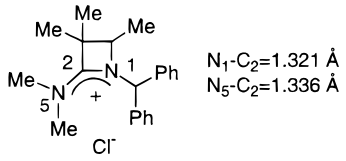

to that found at the B3LYP/6-31G* level. In this local minimum, the C3 and C4 atoms are almost antiperiplanar to each other, as is reflected in the ω values. However, this intermediate has a significant conformational freedom around the N1−C2 bond, and it is expected that in more substituted analogues this antiperiplanar arrangement can vary substantially.

The transition structure leading to the formation of the C3−C4 bond is denoted as **TS2a** in Figure 2, and its chief geometric features are also collected in Figure 3. This saddle point corresponds to a electrocyclic ring closure and connects **INT2a** and **3a** via rotation around the N1−C2 bond and conrotatory torsion around the C2−C3 and N1−C4 bonds. Inspection of the FMO's of **TS2a** reveals that they arise from the bonding and antibonding combination of the HOMO of an enamine and the π^* orbital of an iminic double bond (see Figure 1 of the Supporting Information). Therefore, although the composition of these FMO's is different from that of the transition structure associated with the conrotatory electrocyclic ring opening of cyclobutane, the distorted σ and σ^* combination between C3 and C4 will give rise to torquoelectronic effects[35] (vide infra). The energy barrier associated with this second step is calculated to be 22.08 kcal/mol at the MP2/6-31G*//HF/6-31G* level (Table 1), a value similar to that found using the B3LYP/6-31G* and MP2/6-31G* methods. Since the C3 and C4 atoms are stereogenic and the barrier leading to the C3−C4 bond formation is larger than that associated with the formation of the N1−C2 bond, it is concluded that the second step of the [2 + 2] cycloaddition between keteniminium cations and imines determines the stereochemical outcome of the reaction.

The product of the reaction between **1a** and **2a** is **3a** and its main geometric features are depicted in Figure 3. It is noteworthy that the N1−C2 and N5−C2 bond distances are quite similar. Indeed, the B_{12} and B_{25} bond indices are calculated to be ca. 1.4, thus suggesting that the contribution of the mesomers **3′** (see Scheme 3) is very significant in azetidinium salts. To verify this finding, we performed a search in the Cambridge Structural Database (CSD) using the QUEST3D and PLUTO programs.[36] We found a structure denoted as *COTNAA* in CSD (Scheme 4), which corresponds to a highly substituted 2-azetidinium chloride.[37] In this compound, the N1−C2 bond distance is even slightly *shorter* than the N5−C2 distance, with no appreciable contact between the chloride anion and the nitrogen atoms. The high contribution of the **3′** mesomer, even higher than that computed by us for **3a**, can be motivated by the highly donating character of the benzhydryl group at N1.

To verify the general features of the reaction and in particular that its second step determines the stereochemical outcome, we studied the reaction between *N*,*N*-dimethylketeniminium cation **1b** and **2a** (Chart 1). The stationary points located in the HF/6-31G* and B3LYP/6-31G* energy hypersurfaces are collected in Figure 4. In this case, the HF/6-31G* energy hypersurface was explored by means of IRC calculations (see Figure 2 of the Supporting Information). In addition, given the similarity between the MP2/6-31G* and B3LYP/6-31G*

(35) Dolbier, W. R., Jr.; Korionak, H.; Houk, K. N.; Sheu, C. *Acc. Chem. Res.* **1996**, , *29*, 471 and previous references therein.

(36) *CSD User Manuals*; Cambridge Crystallographic Data Centre, 12 Union Road, Cambridge, UK.

(37) Stierli, F.; Prewo, R.; Bieri, J. H.; Heimgartner, H. *Helv. Chim. Acta* **1984**, *67*, 927.

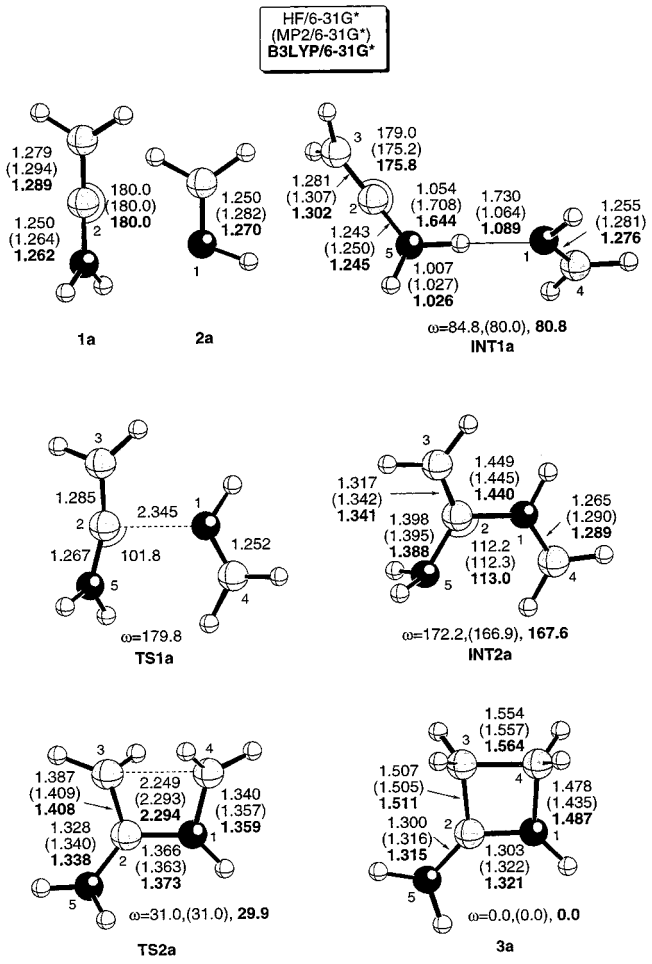

Figure 3. Ball and stick representation of the stationary points found in the reaction between keteniminium cation **1a** and methanimine **2a**. Bond distances and angles are given in Å and deg, respectively. The dihedral angles ω = N1−C2−C3−C4 are given in absolute values. In this and in the subsequents figures that include ball-and-stick representations, unless otherwise stated, atoms are represented by increasing order of shading as follows: H, C, N.

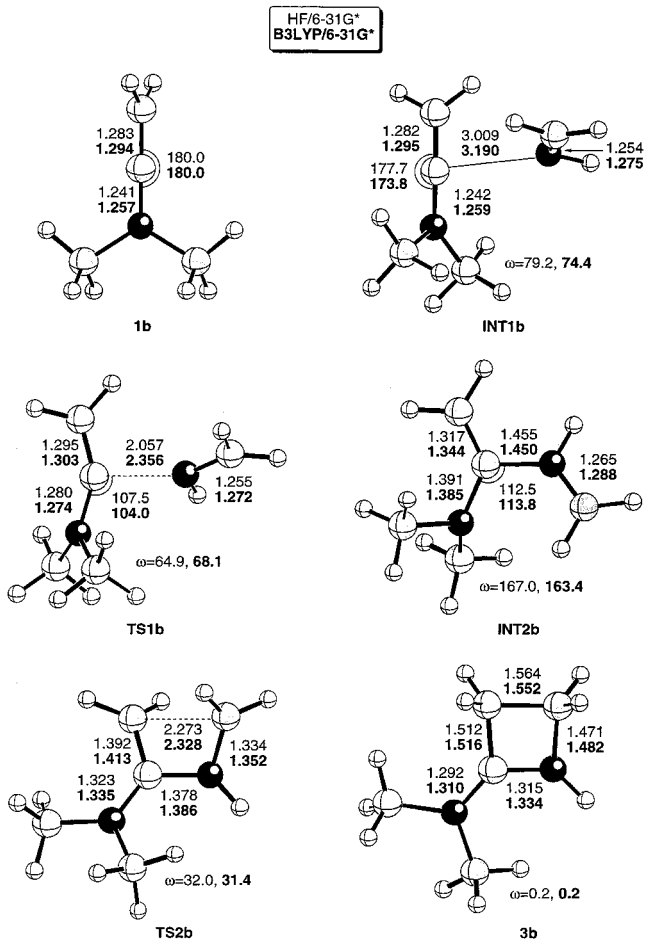

Figure 4. Ball and stick representation of the stationary points found in the reaction between keteniminium cation **1b** and **2a**. See Figure 3 caption for additional details.

results in the parent reaction, electron correlation was explored only at the latter level. The shape of the ion−molecule complex **INT1b** is very different from **INT1a**, since in the former there is not hydrogen bonding between **1b** and **2a**. Therefore, the complexation energy is 10.80 kcal/mol at the B3LYP/6-31G* level (see Table 1). When solvent effects are considered the ΔE_1 value is ca. 6 kcal/mol lower. The first transition structure **TS1b** was located at both the HF/6-31G* and B3LYP/6-31G* levels. The ω values in both **INT1b** and **TS1b** reveal an almost orthogonal approach between both reactants. The first activation barrier associated with the formation of the N1−C2 bond is calculated to be only 0.67 and 0.54 kcal/mol at the B3LYP/6-31G* and B3LYP(SCIPCM)/6-31G* levels, respectively. This result confirms that the stereocontrol of the reaction lies in the second step, namely the formation of the C3−C4 bond. The second reaction intermediate **INT2b** and the second transition structure **TS2b** are quite similar to the analogues found in the **1a** + **2a** → **3a** process. The second barrier of the **1b** + **2a** → **3b** reaction is computed to be 16.68 kcal/mol at the B3LYP/6-31G* level. This value is 3.27 kcal/mol higher when solvent effects are taken into account because of the lower polar character of **TS2b** with respect to **INT2b** (see Table 1). In these processes, a significant amount of the positive charge of the keteniminium cation is transferred to the imine moiety when the N1−C2 bond is formed, which is then redistributed in the course of the second step (see Table 1 of the Supporting Information).

The next step in our study was to determine the reaction profiles for the reaction between an unsymmetrically substituted keteniminium cation as chloroketeniminium cation **1c** and an (*E*)-imine such as (*E*)-ethylideneamine **2b** (see Chart 1). We considered only the (*E*)-isomer of this latter compound, since this is the usual stereochemistry in acyclic imines.[6e,38] In this case, the LUMO plane of the keteniminium cation determines two nonequivalent modes of attack of a nucleophile. If this latter reactant approaches to the cumulene along the side in which the large substituent is located (R_L in Figure 5A), this approach is termed endo attack. If the interaction takes place along the opposite side, then an exo attack takes place. As a consequence, the endo/exo approaches give rise to two intermediates, denoted as *endo*- and *exo*-**INT2c** in Scheme 5.

In the course of the second step, the geometry of the conrotatory transition states imposes the nonequivalence of the four possible positions at the C3 and C4 atoms (see

(38) For recent examples, see: (a) Guerra, A.; Lunazzi, L. *J. Org. Chem.* **1995**, *60*, 7959. (b) Alvaro, G.; Boga, C.; Savoia, D.; Umani-Ronchi, A. *J. Chem. Soc., Perkin Trans. 1* **1996**, 875.

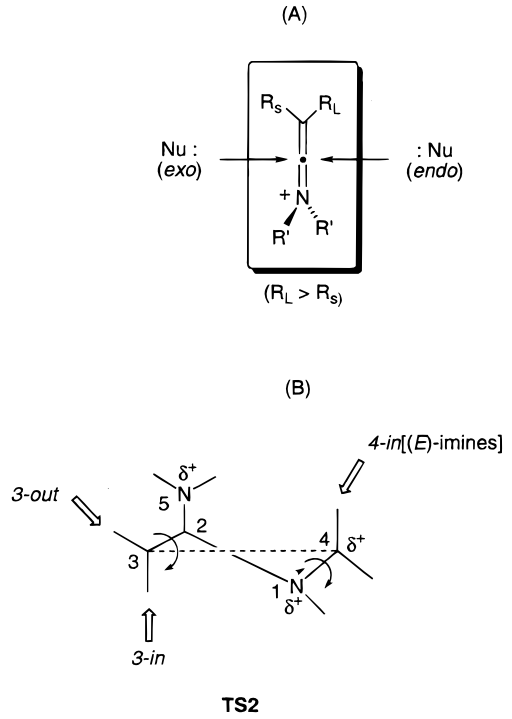

Figure 5. (A) Schematic representation of the two possible modes of the addition of a nucleophile to an keteniminium cation along the LUMO plane. (B) General shape of the second transition state of the [2 + 2] cycloaddition between keteniminium cations and imines.

Scheme 5. Possible Reaction Paths in the Formation of Cis and Trans Cycloadducts 3c

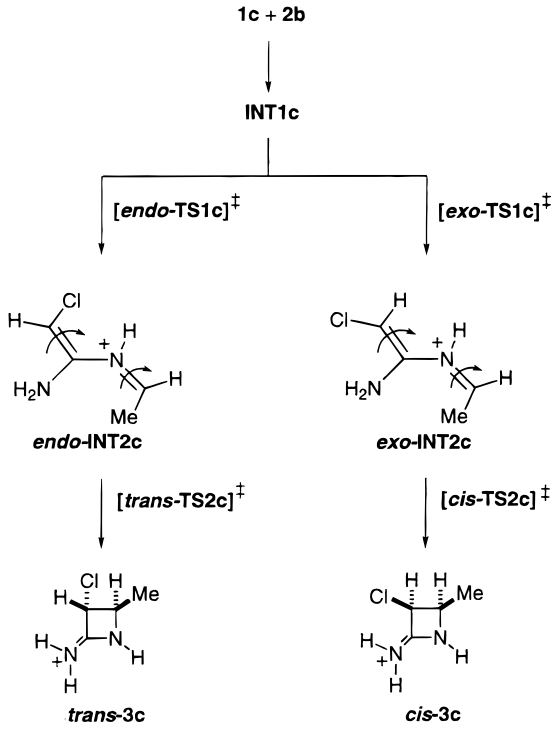

Figure 5B). According to the terminology introduced by Houk,[39] the (*E*)-geometry of the starting imine determines that in the corresponding **TS2** the methyl group of **2b** will occupy the 4-*in* position (Figure 5B). However, the position of the C3-substituent in **TS2** will depend on the mode of attack followed in the first step. Thus, if the N1−C2 bond formation takes place via an exo attack, the substituent at C3 will occupy the *3-out* position, whereas in the case of an endo attack the same substituent will occupy the *3-in* position.[6a] With these considerations in mind, we explored the reaction profiles for the interaction between **1c** and **2b** to yield *cis*- and *trans*-**3c** (see Schemes 5 and 6 and Table 1).

Scheme 6. Kinetic Scheme of the Reaction between 1c and 2b To Form Cycloadducts *cis*- and *trans*-3c

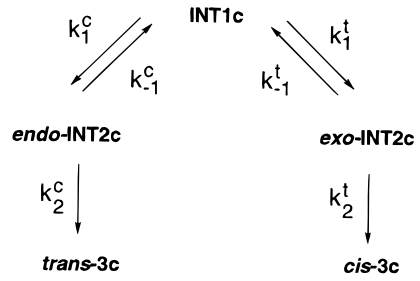

We have used the kinetic equations indicated in Scheme 6 to estimate the cis/trans ratio of cycloadducts **3c**. From our computational studies and the experimental evidence,[16] the steady-state approximation[40] can be applied to intermediates *endo*- and *exo*-**INT2c** since the following expression can be written:

$$[exo\text{-}\mathbf{INT2c}] + [endo\text{-}\mathbf{INT2c}] \ll [\mathbf{1b}] + [\mathbf{2b}] + [cis\text{-}\mathbf{3c}] + [trans\text{-}\mathbf{3c}] \quad (1)$$

In addition, given that $k^{c}_{-1} \gg k^{c}_{2}$ and $k^{t}_{-1} \gg k^{t}_{2}$ (Scheme 6), the cis/trans ratio can be approximated as

$$\frac{[cis\text{-}\mathbf{3c}]}{[trans\text{-}\mathbf{3c}]} = \frac{k^{c}_{2}}{k^{t}_{2}}K \quad (2)$$

where

$$K = \frac{k^{c}_{1}k^{t}_{-1}}{k^{c}_{-1}k^{t}_{1}} = \frac{[exo\text{-}\mathbf{INT2c}]}{[endo\text{-}\mathbf{INT2c}]} \quad (3)$$

Therefore, according to eq 2 the second step of the reaction and the equilibration between the reaction intermediates[41] determine the stereocontrol of the reaction under kinetic control. From the data reported in Table 1 and using the Eyring theory,[40] we have obtained a [*cis*-**3c**]/[*trans*-**3c**] value of 1.7×10^{10} at the MP2/6-31G*//HF/6-31G*+ΔZPVE level. This very large value derives mainly from the energy difference between the ΔE_{a2} values associated with the conrotatory steps *exo*-**INT2c** → *cis*-**3c** and *endo*-**INT2c** → *trans*-**3c**. In addition, following a recommendation made by one reviewer, we have also studied the formation of intermediates *endo*- and *exo*-**INT2d**, corresponding to the interaction between **1d** and (E)-imine **2b** (see Chart 1):

(39) (a) Houk, K. N. In *Strain and its Implications in Organic Chemistry*; de Mejijere, A., Blechert, S., Eds.; Kluwer Academic Publishers: Dordrecht, 1989; p 25. (b) Niwayama, S.; Kallel, E. A.; Spellmeyer, D. C.; Sheu, C.; Houk, K. N. *J. Org. Chem.* **1996**, *61*, 2813.

(40) Espenson, J. H. *Chemical Kinetics and Reaction Mechanisms*; McGraw-Hill: New York, 1981; pp 72−75, 153−156.

(41) We are grateful to one reviewer for suggesting the possible effect of this equilibration between both intermediates on the stereochemical outcome.

Table 2. Relative Energies (kcal/mol) between *cis*- and *trans*-TS2c and -TS2′c

	ΔE_{rel}[a]		$\Delta E'_{rel}$[b]	
method	**cis-TS2c**	**trans-TS2c**	**cis-TS2′c**	**trans-TS2′c**
HF/6-31G*[c]	0.00	+11.03	0.00	+11.04
MP2/6-31G*[c]	0.00	+13.82	0.00	+11.04
B3LYP/6-31G*[d]	0.00	+12.94	0.00	+11.20
B3LYP(SCIPCM)/6-31G*[d]	0.00	+12.33	0.00	+10.97

[a] Relative energies with respect to *cis*-**TS2c**. [b] Relative energies with respect to *cis*-**TS2′c**. [c] Energy computed on HF/6-31G* fully optimized geometry. The ZPVE correction, conveniently scaled and calculated at the same level, has been included. [d] Energy computed on B3LYP/6-31G* fully optimized geometry. The ZPVE correction has been included.

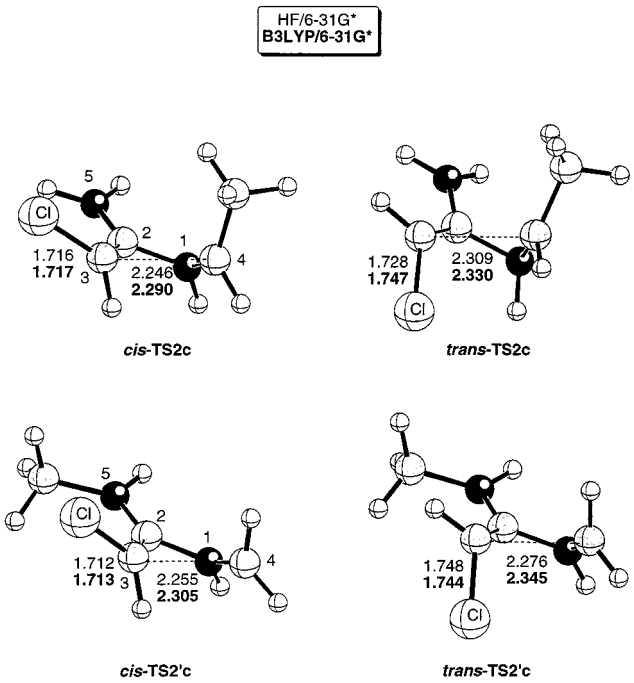

Figure 6. Ball and stick representation of transition structures **TS2c** and **TS2′c**. See Figure 3 caption for additional details.

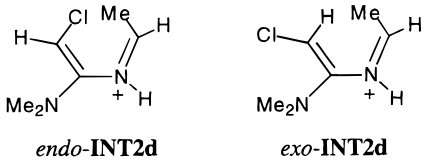

The corresponding stationary points located at the HF/6-31G* level are reported in Figure 4 of the Supporting Information. According to our results, these intermediates are formed from the reactants with no activation barrier (MP2/6-31G*//HF/6-31G*+ΔZPVE results, see the Supporting Information). Therefore, the stereochemical outcome of this reaction in more substituted systems depends solely on the conrotatory step and on the equilibrium between the possible diastereomeric intermediates **INT2**. Therefore, since only the second transition structures of this reaction are stereochemically relevant,[41] the subsequent discussion will be restricted to these saddle points. The chief geometric features of the remaining stationary points are reported in Figure 3 of the Supporting Information.

The two possible transition structures associated with the formation of *cis*- and *trans*-**3c** are depicted in Figure 6, and the respective relative energies are reported in Table 2. We have found that *cis*-**TS2c** is of much lower energy than its trans analogue at all the levels of theory included in our study. For example, at the B3LYP/6-31G* level *trans*-**TS2c** is 12.94 kcal/mol less stable than *cis*-**TS2c**. This value is similar to the difference found by Houk et al.[39b] for the electrocyclic ring cleavage of 2-chlorocyclobutene. Moreover, this difference is not substantially modified by inclusion of solvent effects, as seen in the SCIPCM values reported in Table 2. Since in experimental studies the N5 atom incorporates alkyl substituents, we have also performed similar calculations locating the methyl group at N5 instead of at C4. The resulting transition structures have been denoted as *cis*- and *trans*-**TS2′c** (see Figure 6). From the $\Delta E'_{rel}$ values reported in Table 2, it is clear that the *N*-methyl group does not modify substantially the energy difference between the saddle points having 3-*in* and 3-*out* chlorine atoms. It is also noteworthy that in *cis*- and *trans*-**TS2c** the C3−Cl bond distances are different. Thus, in *trans*-**TS2c**, which incorporates one 3-*in* chlorine atom, this distance is calculated to be 0.03 Å larger than that of its cis analogue (see Figure 6). According to the torquoelectronic theory,[39] this enlargement minimizes the repulsive interactions between a lone pair of the *in*-3-Cl atom and the C3−C4 bond in formation (Scheme 7). In addition, the NPA of trans-**TS2c** shows that at the HF/6-31G* level there is a $\pi_{2,5} \rightarrow \sigma^*_{3,Cl}$ donation whose second-order perturbation energy is −2.87 kcal/mol (Scheme 8). Similarly, at the same level, the NPA assigns a π-lone pair of electrons to the C_3 atom, and the donation from a lone pair of electrons of the chlorine atom is calculated to be 6.45 kcal/mol more efficient in *cis*-**TS2c** (Scheme 8).

Scheme 7. Main Stereoelectronic Interactions Operating in the Conrotatory Transition Structure Including an *Inward* Chlorine Atom

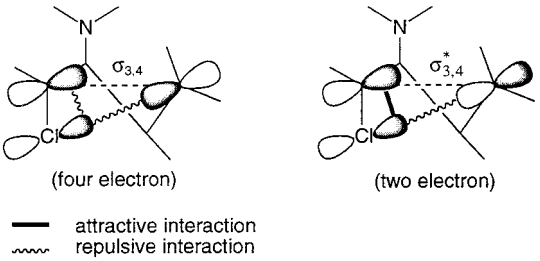

In summary, if only torquoelectronic effects are considered, virtually exclusive formation of *cis*-2-azetidinium salts is predicted. From the data reported in the literature, it is found that this is indeed the case when triflic anhydride and *N*,*N*-dialkylcarboxamides are used as starting materials. Moreover, Battaglia et al. have shown that under the reaction conditions there is no detectable epimerization at the C3 position of the cycloadducts.[16] In contrast, when phosgene is used to generate the electrophilic species, preferential or exclusive formation of *trans*-2-azetidinium salts is observed[14] (Scheme 9). These latter experimental results are not in agreement with the results exposed above.

Scheme 8. Main HF/6-31G* Second-Order Perturbational Energies in *cis*- and *trans*-TS2c, According to the Natural Population Analysis

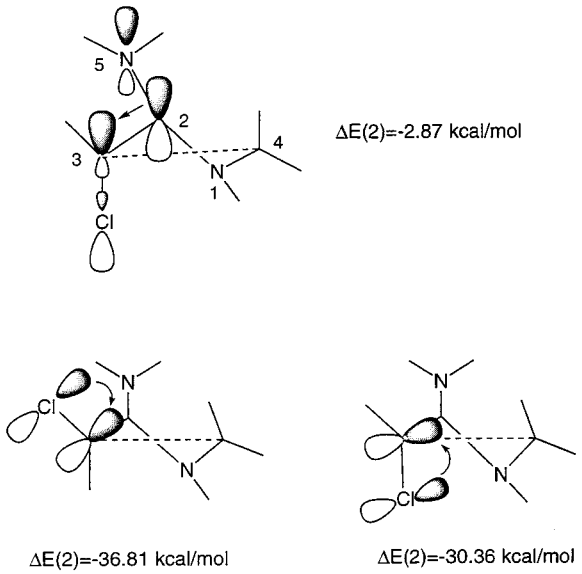

Scheme 9. Stereodivergent Synthesis of *cis*- and *trans*-2-Azetidinium Salts

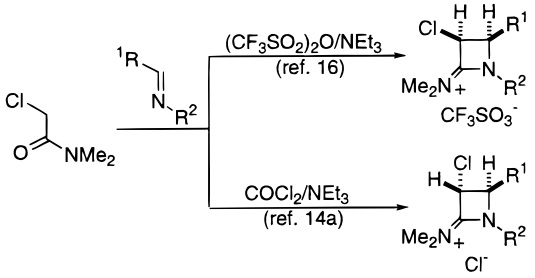

Chart 2

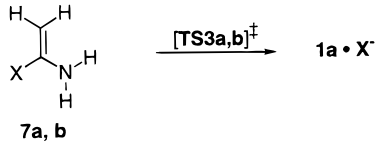

7a, b

7a: X=Cl
7b: X=CF_3SO_3

To understand the origins of the different stereochemical outcome of the reaction depending upon the method used to generate the electrophilic species, we have computed the formation of keteniminium salts **1a** from enamines **7a,b** (X = Cl, TfO) (Chart 2). The fully optimized geometries of these latter compounds as well as those of the corresponding transition structures **TS3a,b** are reported in Figure 7. The activation energies computed at different theoretical levels are reported in Table 3. Since in the formation of the keteniminium salts ionic pairs are generated from neutral substrates, these reactions are strongly solvent dependent. Thus, in **TS3a** there is an almost complete charge separation between the chlorine atom and the keteniminium cation **1a** in the gas phase, with a NPA charge of −0.914 at the HF/6-31G* level for the chlorine atom. When solvent effects are taken into account, this value drops to −0.870 (see Figure 7), and the Cl···C bond distance is calculated to be ca. 0.17 Å shorter than in the gas phase at the same level.

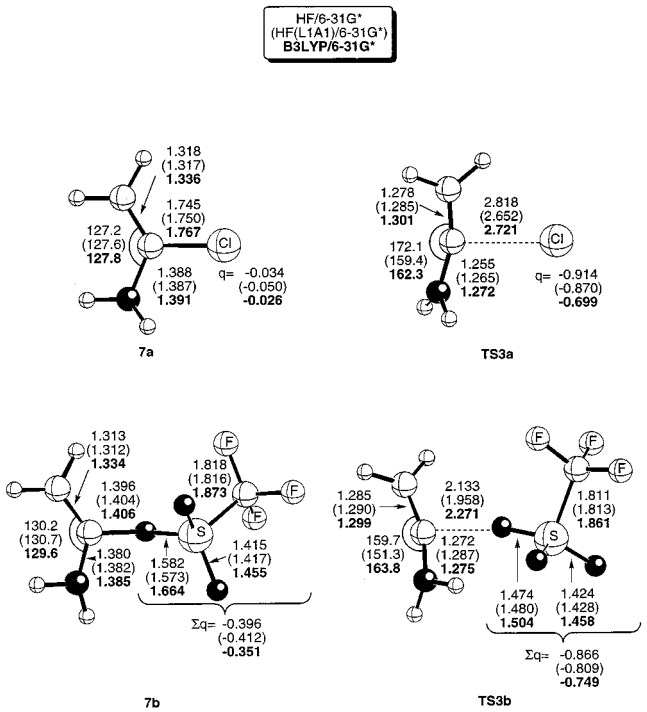

Figure 7. Ball and stick representation of enamines **7a,b** and the transition structures leading to **1a** (see Chart 2). See Figure 3 caption for additional details. $\sum q$ stands for the NPA charge of the anionic moiety (chloride or triflate).

Table 3. In Vacuo (ε = 1.00) and 1,2-Dichloroethane (ε = 10.37) Activation Energies[a] (ΔE_{a3}, kcal/mol) Associated with the Reactions Included in Chart 2

method	ΔE_{a3} X = Cl	ΔE_{a3} X = TfO
	ε = 1.00	
HF/6-31G*[b]	40.00	18.92
MP2/6-31G*[b]	50.78	21.05
B3LYP/6-31G*[c]	36.56	18.17
	ε = 10.37	
HF(L1A1)/6-31G*[d]	23.19	12.91
MP2(L1A1)/6-31G*[d]	34.30	14.02
B3LYP(SCIPCM)/6-31G*[c]	26.77	13.50

[a] ZPVE corrections, computed at the level of the geometry optimization, have been included. [b] Geometry optimized at the HF/6-31G* level. [c] Geometry optimized at the B3LYP/6-31G* level. [d] Geometry optimized at the HF(L1A1)/6-31G* level.

Since **TS3a** is found to be earlier in solution than in the gas phase, it is expected that the activation energy for this process should be lower in the former case. According to the results reported in Table 3, this is indeed the case. For instance, the ΔE_{a3} value for **TS3a** is found to be 16.48 kcal/mol lower in 1,2-dichloroethane solution than in the gas phase at the MP2/6-31G* level. Therefore, the ΔE_{a3} values associated with the **7a** → **1a**·Cl^- reaction are larger than those found for the **1a** + **2a** → **3a** process (see Tables 1 and 3). In other words, if chloroenamines are used as precursors of the corresponding keteniminium salts, the formation of these electrophilic species is the limiting step of the whole process. In the case of trifluoromethane−sulfonate enamine **7b**, the general features of **TS3b** reveal that this latter saddle point is quite similar to **TS3a** (see Figure 7). However, the highly polarizable triflate moiety induces a significantly lower activation energy, as is seen in the ΔE_{a3} values for X = TfO in Table 3. In particular, the ΔE_{a3} values are now

Table 4. Relative Energies for the Transformations Depicted in Chart 3[a]

method	8a → TS4a	8a → TS5a	TS5a → INT2a·Cl⁻	INT2a·Cl⁻ → TS2a·Cl⁻
HF/6-31G*[b]	+52.90	+23.05	−12.52	+36.80
MP2/6-31G*[b]	+50.80	+35.57	−17.36	+25.95
B3LYP/6-31G*[c]	+41.30	+25.54		
HF(L1A1)/6-31G*[d]		+5.91	−8.52	+37.98
MP2(L1A1)/6-31G*[d]		+11.81	−5.74	+28.29
B3LYP(L1A1)/6-31G*[e]	+29.89	+7.50	−6.21	+26.98
B3LYP(SCIPCM)/6-31G*[e]	+29.79	+3.50	−4.96	+26.62

[a] See Figure 8 for the geometrical features of these stationary points. The corresponding ZPVEcorrections, computed at the optimization level, have been included. [b] Geometries optimized at the HF/6-31G* level. [c] Geometries optimized at the B3LYP/6-31G* level. [d] Geometries optimized at the HF/(L1A1)/6-31G* level. [e] Geometries optimized at the B3LYP(L1A1)/6-31G* level.

Chart 3

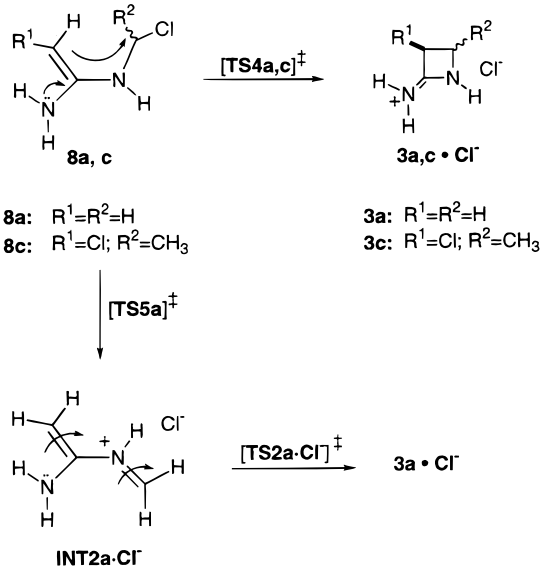

lower than the ΔE_{a2} values found for the **1a** + **2a** → **3a** process (see Table 1). Therefore, the trifluoromethanesulfonate enamines can follow the keteniminium salt−imine route and are subjected to the strict cis stereocontrol imposed by torquoelectronic effects. The final result is that in this case cis cycloadducts will be obtained, in good agreement with the experimental findings (vide supra).

According to Scheme 3, if chloroenamines generated from *N*,*N*-dialkylcarboxamides and phosgene can avoid the two-step [2 + 2] route, the intermediate alkyl chlorides **8** could be formed. Therefore, we have explored the possible reaction paths of intermediate **8a**, which are depicted in Chart 3. The chief geometric features of the stationary points found are shown in Figure 8, and the computed energy differences for the steps which interconnect them are reported in Table 4. Intermediate **8a** is calculated to exist mainly in the conformation in which the N1 lone pair and the C−Cl bond are antiperiplanar to each other. We have also located the transition structure associated with the formation of the C−Cl bond. This saddle point is denoted as **TS5a** in Chart 3, and its geometrical features are depicted in Figure 8. **TS5a** lies 25.54 kcal/mol above **8a** at the B3LYP level in the gas phase (Table 4). An IRC calculation from **TS5a** leads to **8a** and to **INT2a·Cl⁻**, whose geometric features are also reported in Figure 8 (see Figure 5 of the Supporting Information).[42] In solution, the activation barriers corresponding to the **INT2a·Cl⁻** → **8a** interaction are substantially lower, given the highly polar character of **TS5a** (see Table 4). Therefore, we can conclude that the

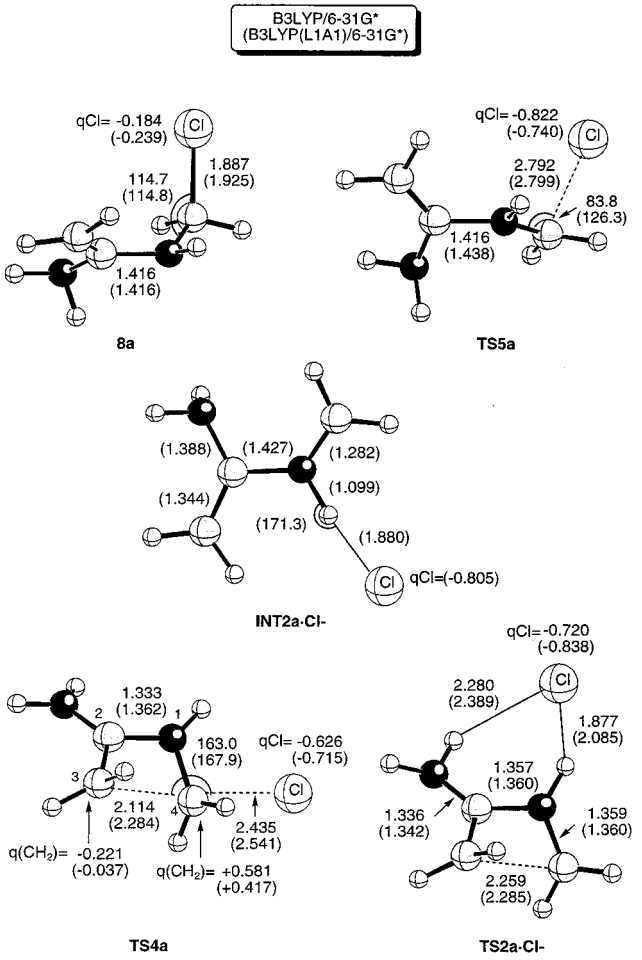

Figure 8. Ball and stick representation of the stationary points included in Chart 3. See Figure 3 caption for additional details. *q* stands for the NPA charge of the corresponding atom or group.

9 → **8** transformation depicted in Scheme 3 is quite facile in solution when X = Cl.

We have also investigated the transformation **8** → **3a·Cl⁻** (see Chart 3). According to the Baldwin rules for cyclization, this intramolecular S_N2 reaction is a favored [4-*exo*-*tet*] process, in which the nucleophile is the enamine moiety of **8** and the chlorine atom is the leaving group. We have located the **TS4a** saddle point that connects **8a** with **3a·Cl⁻** (Figure 8). This saddle point exhibits some of the usual features of those associated with more conventional S_N2 reactions (see, for instance,

(42) Mayr, Würthwein, et al. have recently reported a combined NMR and computational study that supports this structure for iminium ion pairs. See: Mayr, H.; Ofial, A. R.; Würthwein, E.-U.; Aust, N. C. *J. Am. Chem. Soc.* **1997**, *119*, 12727.

the FMO's of **TS4a** in Figure 6 of the Supporting Information).[43] However, a substantial departure from the linear arrangement between the nucleophilic atom C3 and the leaving group is observed. (see Figure 8). Streitwieser[44] and Bader[45] have reported that the ipso carbon atom in this kind of transition structures has strong ionic character. In our case, the NPA charge of C4 (including the two hydrogen atoms) is +0.581 at the B3LYP/6-31G* level (Figure 8). Since the charge of the chlorine atom is −0.626 at the same level, this indicates that in **TS4a** most of the positive charge of the 2-azetidinium cation is located at the C4 atom. Given the highly polar character of **TS4a**, their geometric and energetic features change substantially when solvent effects were taken into account (Figure 8). At the HF(L1A1)/6-31G* level, this saddle point could not be located. Upon optimization it spontaneously converged to the products. However, at the B3LYP(L1A1)/6-31G* level **TS4a** was located and characterized, and their geometric features did not vary substantially from those calculated in vacuo (see Figure 8). The activation energy associated with the **8a** → **3a·Cl**$^-$ process was found to change dramatically on passing from the gas phase to the solution. Thus, at the B3LYP/6-31G* this energy barrier was calculated to be 41.3 kcal/mol (Table 4). However, at the B3LYP(L1A1)/6-31G* level this value is calculated to be ca. 11.4 kcal/mol lower (see Table 4).

To compare the intramolecular S_N2 process with the conrotatory electrocyclization, we have also computed the effect of a chlorine anion on **TS2a**. As it can be seen from inspection of Figure 8, in **TS2a·Cl**$^-$ the anion forms two hydrogen bonds with the N1−H and N5−H moieties. However, since in practice these two nitrogen atoms are substituted, these hydrogen bonds (and that of **INT2a·Cl**$^-$) are not chemically relevant. The activation barrier associated with the conrotatory ring closure is computed to be ca. 3 kcal/mol lower in energy than the S_N2 process at the B3LYP(L1A1)/6-31G* level (see Table 4). However, aside from the stabilizing electrostatic interaction between **TS2** and the chloride anion, the stabilizing hydrogen bonds in **TS2·Cl**$^-$, which are *not* present in real reactants, must be discounted. For instance, the experimental energy of anion−amine hydrogen bonds is reported to be ca. 5−10 kcal/mol.[46] Therefore, within the limitations of our simplified computational models, we can conclude that in the presence of chloride anions the system follows preferentially the S_N2 pathway.

Finally, we have computed the relative energies of the [4-*exo*-*tet*] transition structures leading to the formation of *cis*- and *trans*-3-chloro-4-methylazetidinium chlorides **3c·Cl**$^-$ (Chart 3). In principle, since **TS4a** has C_1 symmetry, four stereoisomeric transition structures can be expected. However, of these four, only two were obtained when the corresponding starting geometries were optimized. These transition structures, denoted as *cis*- and *trans*-**TS4c**, together with their respective relative energies, are reported in Figure 9. From these data, it is clear that the stereocontrol in the intramolecular S_N2 process

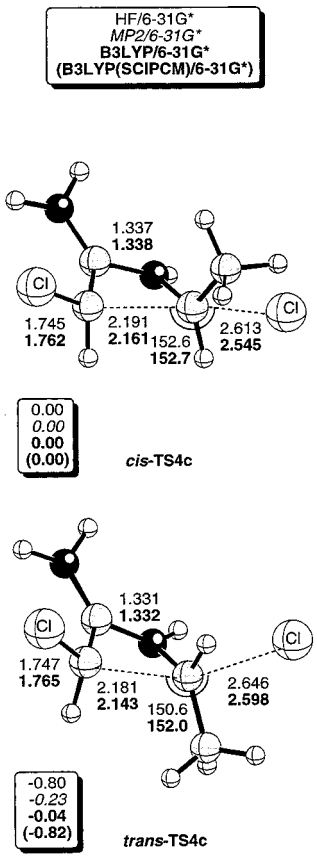

Figure 9. Ball and stick representation of transition structures *cis*- and *trans*-**TS4c**. See Figure 3 caption for additional details. Numbers in boxes are the relative energies in kcal/mol. The MP2/6-31G* and B3LYP(SCIPCM)6-31G* energies have been computed on fully optimized HF/6-31G* and B3LYP/6-31G* geometries, respectively. The corresponding ZPVE corrections have been included.

is much lower than that imposed by torquoelectronic effects. Thus, at the B3LYP/6-31G* level the difference in energy between both transition structures is virtually negligible. When solvent effects are estimated by means of the SCIPCM approximation, preferential formation of the *trans*-2-azetidinium chloride is predicted. This result is in agreement with the observations of Ghosez et al.,[14] in which the electrophilic species are generated in the presence of chloride anions, thus promoting preferential formation of trans cycloadducts with low stereocontrol.

Conclusions

From the computational studies reported in the present work, the following conclusions can be drawn:

(i) The reaction between keteniminium cations and imines is stepwise, the former step being the formation of the N1−C2 bond, followed by electrocyclic ring closure to form the C3−C4 bond.

(ii) The stereocontrol of reaction between keteniminium cations and imines is determined by the second step of the reaction and is subjected to torquoelectronic effects. The preferential transition structure for an (*E*)-imine is that leads to the corresponding cis cycloadduct, as indicated in Scheme 10.

(iii) The stereochemistry of the reaction between keteniminium cations and imines depends on the nature of the anion, which in turn is related to the method used

(43) Shaik, S. S.; Schlegel, H. B.; Wolfe, S. *Theoretical Aspects of Physical Organic Chemistry, the S_N2 Mechanism*; John Wiley and Sons: New York, 1992.

(44) (a) Streitwieser, A.; ChoY, G. S.-C.; Abu-Hasanayn, F. *J. Am. Chem. Soc.* **1997**, *119*, 5013. (b) Wiberg, K. B.; Schleyer, P. v. R.; Streitwieser, A. *Can. J. Chem.* **1996**, *74*, 892.

(45) Bader, R. F. W. *Can. J. Chem.* **1986**, *64*, 1036.

(46) Ash, E. L.; Sudmeier, J. L.; De Fabo, E. C.; Bachovchin, W. W. *Science* **1997**, *278*, 1128.

Scheme 10. General Shape of the $[\pi]_c^4$ Transition State Associated with the Second Step in the Reaction between Keteniminium Salts and Imines

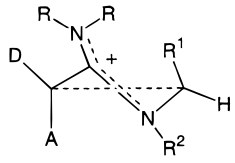

D≡ Donor group
A≡ Acceptor group

Scheme 11. General Shape of the [4-*exo*-*tet*] Transition State Associated with the Formation of the C3−C4 Bond

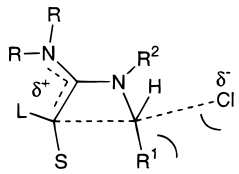

L≡ Large substituent
S≡ Small substituent

in the generation of the keteniminium species. If a nucleophilic anion such as chloride is present in the reaction medium, the formation of the C3−C4 bond can preferentially take place via intramolecular S_N2 reactions. The transition states associated with these [4-*exo*-*tet*] processes have the general shape depicted in Scheme 11. This reaction path leads to the preferential formation of trans cycloadducts, in which the L and R^1 substituents are away to each other.

(iv) Torquoelectronic effects promote a stereocontrol larger than that observed in [4-*exo*-*tet*] processes. To favor the conrotatory electrocyclization, highly polarizable nonnucleophilic anions must be used to generate the keteniminium cation. Addition of reagents capable to remove nucleophilic anions from the reaction medium can also be considered.

Acknowledgment. The present work has been supported by the Gobierno Vasco/Eusko Jaurlaritza (Project GV 170.215-EX97/11) and by the Secretaría de Estado de Universidades, Investigación y Desarrollo (Project PB96-1481). We are also grateful to the CIEMAT for a generous gift of computing time on the CRAY YMP-EL computer.

Supporting Information Available: Table including the total energies and zero-point vibrational energies (in atomic units) of all stationary points discussed in the text. Table including the bond indices and NPA charges of the stationary points found in the reaction between **1a,b** and **2a**. Figures including FMO's of transition structures **TS2a** and **TS4a**. Figures showing the energy profiles of the IRC calculations on the **1b** + **2a** → **3b** and **8a** → **INT2a·Cl** processes. Figure showing the chief geometric features of the stationary points corresponding to the **1c** + **2b** → **3c** reaction. Figure showing the chief geometric features of the first stages of the interaction between **1d** and **2c**. This material is available free of charge via the Internet at http://pubs.acs.org.

JO9815002